A Frequency-Domain Approach to Analysing Dynamic Deep Stall Recovery

Duc H. Nguyen[1], Mark H. Lowenberg[2], and Simon A. Neild[3]
Department of Aerospace Engineering, University of Bristol, Bristol, BS8 1TR

Although the problem of locked-in deep stall is well known and has a long history, there currently exists no consistent procedure that can guarantee recovery. Past studies have suggested that it might be possible to rock the aircraft nose to destabilise the stable deep stall trim point, thereby gaining enough momentum to push the nose down. However, the methods used in these studies are either of preliminary or empirical nature and brought inconsistent results. In this paper, we use bifurcation analysis to derive a recovery manoeuvre, specifically by assessing the aircraft's nonlinear frequency response under an elevator forcing. The ensuing nonlinear Bode plot detects unstable (divergent) solutions near resonance that contributes to a successful deep stall recovery. Moreover, the nonlinear resonant frequency is slightly lower than the result obtained using linear analysis, and time simulation shows that relying on the linear result does not lead to a successful recovery. It was also found that at the high angles-of-attack associated with deep stall, the frequency separation between the short period and phugoid mode is significantly reduced, leading to only one visible peak in the frequency response. This feature is also reflected in the time-domain step response.

I. Introduction

Deep stall (also known as super stall) is a dangerous phenomenon in which the aircraft is locked into a high angle-of-attack attitude that results in a steep descending trajectory. In serious cases, this descending trajectory is maintained even with the nose horizontal or pointing upward (i.e., the aircraft falls belly-first – see Fig. 1b). A deep stall is deemed unrecoverable when there is insufficient pitch control authority to bring the nose down and reduce the angle-of-attack. This problem has resulted in several accidents of early T-tail airliners – a design that is especially susceptible to deep stall [1]. Although there are many successful safety measures in use to prevent excursion into the deep stall region, most commonly via stick shaker & stick pusher [1] and digital angle-of-attack limiter in full-authority fly-by-wire systems [2, 3], research into deep stall recovery methods are few and of limited scope. These studies either involve simplified flight dynamics models [4-8] or empirical methods [3, 9], making it hard to determine a safe and consistent procedure to guarantee recovery. Moreover, recent research into advanced landing techniques for small unmanned aerial vehicles involves deliberately bringing the aircraft into a deep stall to minimise the landing distance [10-12]. These developments further emphasise the need to improve our understanding of the flight characteristics in the deep stall regime. Future research into this topic can also benefit from recent data published by NASA [13-15], which provides high-fidelity flight dynamics modelling of a hypothetical T-tail passenger aircraft (the GTT) as part of the global effort to reduce airliners loss-of-control [16, 17]. This model provides aerodynamic data for up to 60º angle-of-attack – well within the deep stall region – whereas reliable aerodynamic data beyond stall is not usually available for many airliner models out there.

The use of bifurcation analysis and continuation methods has proven to be a powerful tool for nonlinear flight dynamics analysis in the past four decades [18-21]. Recent developments in the field saw the use of a harmonic forcing term to generate a 'nonlinear Bode plot', which facilitates assessments of the non-stationary nonlinear elements like sub/super-harmonic resonances [22] and actuator rate limiting [23]. This approach is exploited in this paper to systematically investigate a feasible deep stall recovery strategy. Specifically, previous works have indicated that it is

---
[1] PhD student. AIAA Student Member.
[2] Professor of Flight Dynamics. AIAA Senior Member.
[3] Professor of Nonlinear Structural Dynamics.

possible to rock the aircraft's nose to gain momentum, making it possible to gain some pitch control and push the nose down below the critical angle-of-attack [3, 6, 9]. We therefore hypothesise and then demonstrate that a nonlinear frequency-domain analysis can provide further insights on this problem and help derive a successful recovery manoeuvre.

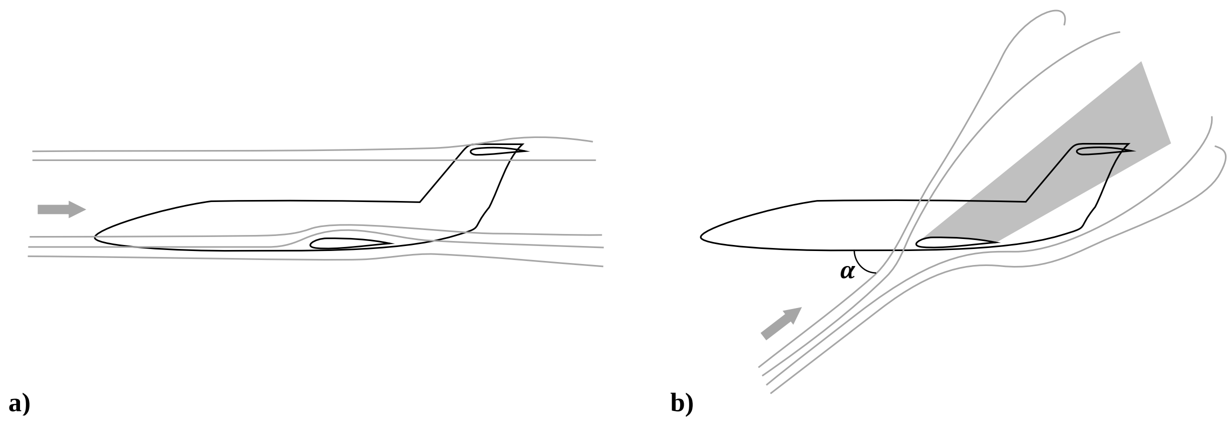

Fig. 1 A T-tail aircraft in normal flight (a) and deep stall (b).*

A brief explanation of the deep stall problem is provided in section II, followed by a review of existing studies on deep stall recovery. Section III describes the aircraft model used for this study. The main result is presented in section IV, and section V provides the concluding remarks. All bifurcation analyses were done in the MATLAB/Simulink environment using the Dynamical Systems Toolbox [24], which is the MATLAB/Simulink implementation of the numerical continuation software AUTO [25].

II. Deep Stall Analysis

The conventional way to predict a deep stall is to examine the relationship between pitching moment coefficient C_M and angle-of-attack α. A trimmed aircraft will have zero pitch rate (q = 0), thereby requiring $C_M = 0$. Because C_M is a function of angle-of-attack, a statically stable trim point has $\frac{\partial C_M}{\partial \alpha} < 0$. Fig. 2 shows an example $C_M(\alpha)$ plot of a T-tail design. The third trim point at 51^{o} angle-of-attack is stable. If there is not enough pitch control authority to bring the nose down, the aircraft will be stuck in this high α condition, leading to an unrecoverable deep stall.

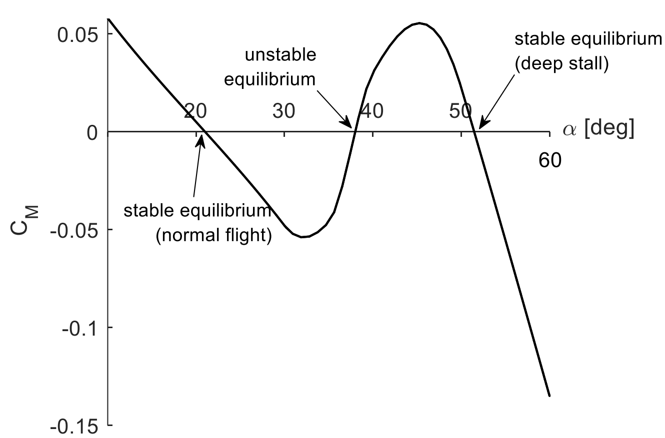

Fig. 2 Typical pitching moment coefficient plot for the T-tail configuration. Negative slope indicates positive static stability in pitch.

**Adapted from en.wikipedia.org/wiki/File:Deep_stall.svg (accessed 26 May 2021)*

Unrecoverable (locked-in) deep stall due to insufficient pitch control power is usually linked to the following features:

- A T-tail configuration, which puts the pitch control devices (elevators and stabilators) in the wake of the wing at high angles-of-attack and render them ineffective (see Fig. 1b).

- An aft centre of gravity, which reduces the elevator/stabilator moment arm. This design is usually found in statically unstable fighter aircraft for improved manoeuvrability and reduced trim drag.

Past studies on deep stall recovery that involved destabilising the aircraft via forcing of the pitch control device are rather empirical and bring mixed results. For example, NASA suggested that upon entering a deep stall, the pilot would observe the transient oscillation as the aircraft settles into the stable high-α trim and pump the stick at the same frequency as that oscillation [3]. The idea is that by matching the forcing input with aircraft's natural rigid-body frequency, it would be possible to build up some momentum with the little control authority available to push the nose down. An earlier study by NASA on a simplified T-tailed airliner model [6] used a somewhat similar idea (referred to as 'dynamic recovery'): the elevator is excited in a square wave pattern, which reverses direction when the pitch rate reaches zero. Both methods require close observation of the ensuing transient oscillation in order to match the forcing input with the aircraft's frequency. In fact, it was noted in [3] that slow or unsuccessful recoveries were attributed to the difficulty of matching the input frequency. There is also the risk of the pilot not reacting fast enough to deep stall entry, meaning that the oscillation is already damped out by the time the pilot initiates the manoeuvre. Furthermore, it was not highlighted in the studies above that the frequency-domain dynamics of the aircraft at such high angles-of-attack is highly nonlinear. Depending on how the aircraft entered the deep stall condition, the ensuing oscillation may have different and varying frequencies, making it more challenging to observe the motion and provide a forcing term.

A different recovery procedure was proposed in [4]. Using an F-16 fighter jet model, it was found that at maximum thrust, the deep stall stable trim point at full nose-down stabilator becomes unstable. However, the time history in [4] shows that it takes 60 seconds of max thrust to take the aircraft out of the deep stall region (i.e., the unstable mode is very slow). The method also demands that the engine produces maximum thrust throughout the entire manoeuvre. This is not a valid assumption as most engines will experience a noticeable performance reduction at such high angles-of-attack or even flame out. In addition, given that there is a publicly-available high-fidelity model of the F-16's engine, we are unable to further pursue this method.

To conclude, forcing the pitch control device to rock the aircraft's nose and generate some nose-down momentum is a promising approach for deep stall recovery. The challenges encountered by previous studies on this method have been highlighted, mostly due to high pilot workload and the complex dynamics at such high angles of attack. Our proposed nonlinear frequency analysis can provide a systematic method to devise a successful escape manoeuvre and overcome the issues discussed above.

III. Aircraft Model

The NASA's Generic T-Tail Transport model (GTT) is used for this study. As the name suggests, this model represents a generic mid-size regional jet airliner with a T-tail configuration. Its aerodynamic data was collected from a series of low-speed sub-scale wind tunnel and water tunnel tests, and some preliminary results have been reported in recent conferences [13-15]. Computational fluid dynamics was also deployed to estimate the influence of Reynolds number on the measured aerodynamics data, allowing corrections to the pitching moment and pitch damping data to be implemented to represent the equivalent full-scale aircraft. For this study, we used this Reynolds-corrected data to construct a 4th-order model that contains only longitudinal motions without flaps and spoilers, which is deemed adequate for this study. All lateral-directional states and inputs are therefore zero. This 4th-order implementation contains 19 aerodynamics tables, which are 1D and 3D functions of angle-of-attack (aoa) and aoa/stabilator/elevator deflections. The valid angle-of-attack range is from –8^o to 60^o.

For pitch control, the GTT uses both stabilator and elevator. It has been reported in [13] that a locked-in deep stall is possible when the centre of gravity is at 40% mean aerodynamic chord (MAC) with the stabilator in full nose-down position (–10^o). This is confirmed by unforced bifurcation analysis. Fig. 3 is a bifurcation diagram showing branches of stable and unstable equilibria solutions over the full physical range of elevator inputs. It indicates that the stable deep stall branch at high angles-of-attack (above 30 deg) extends all the way to δ_e = 20^o – the maximum nose-down elevator position, which is indicative of a locked-in deep stall that agrees with experimental results [13]. The pitch rate bifurcation diagram is not shown in Fig. 3 since all equilibrium solutions have zero pitch rate. For further reference, Fig. 4 shows the pitching moment coefficient at three elevator positions. Due to the lack of an engine model for the GTT, we assume zero thrust for our analysis. At the high angles-of-attack involved in a deep stall, any civil engines will suffer serious performance issues, so the zero thrust assumption corresponds to the worst-case scenario. This will also remove the nose-down moment generated by the high-mounted engines on the GTT, which can affect the outcomes concerning deep stall recovery.

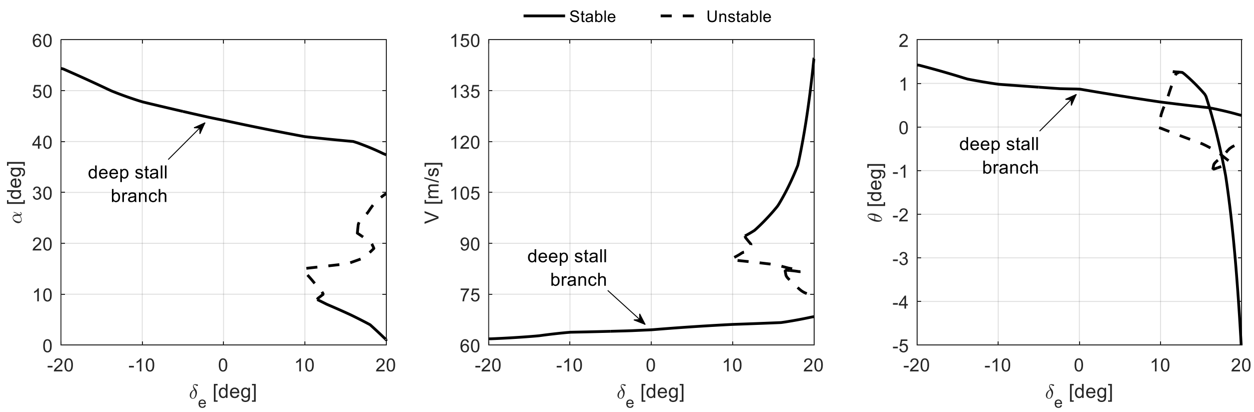

Fig. 3 Bifurcation diagram – elevator continuation at full nose-down stabilator and zero thrust.

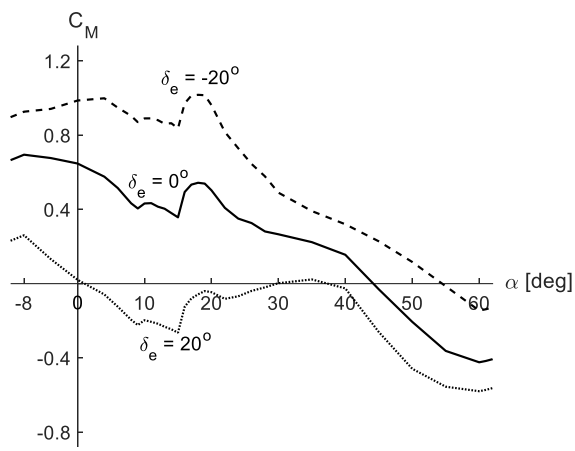

Fig. 4 GTT pitching moment coefficients at full nose-down stabilator.

IV. Results and Discussion

The existence of a locked-in deep stall has been verified by unforced bifurcation analysis. To devise a recovery manoeuvre using nonlinear frequency analysis, we apply a harmonic forcing to the elevator in the form of $\delta_e = 20\sin\omega t$, where 20 is the maximum possible amplitude in degree for stop-to-stop elevator movement and ω is the forcing frequency in rad/s. This replicates the stick pumping action in [4], albeit done in an open-loop manner. Fig. 5 shows the resulting linear and nonlinear Bode plots. The former was generated by numerical continuation using the method defined in [22] while the latter was obtained by linearising the aircraft in deep stall at neutral elevator ($\delta_e = 0^o$). The state-space matrices of the linear model are provided in the appendix. At such a large forcing amplitude of 20^o, it is expected that the linear and nonlinear frequency responses will differ significantly. One of the first notable features is that the nonlinear frequency response leans to the left and has lower resonance frequency comparing to its linear counterpart, indicating a softening system (i.e., the restoring moment becomes weaker as the aircraft moves further away from the deep stall trim point). More importantly, unstable solutions are detected near resonance in the nonlinear response, which can coexist with the stable ones at some frequencies. For ω between 0.29 to 0.51 rad/s, there are only unstable solutions in the nonlinear frequency response. The aircraft forced at one of these frequencies will diverge to infinity. In the context of deep stall recovery, this is desirable as the pilot can gain some momentum from the large-amplitude oscillation, allowing him/her to then push the nose down and bring the aircraft back to the low-α regime.

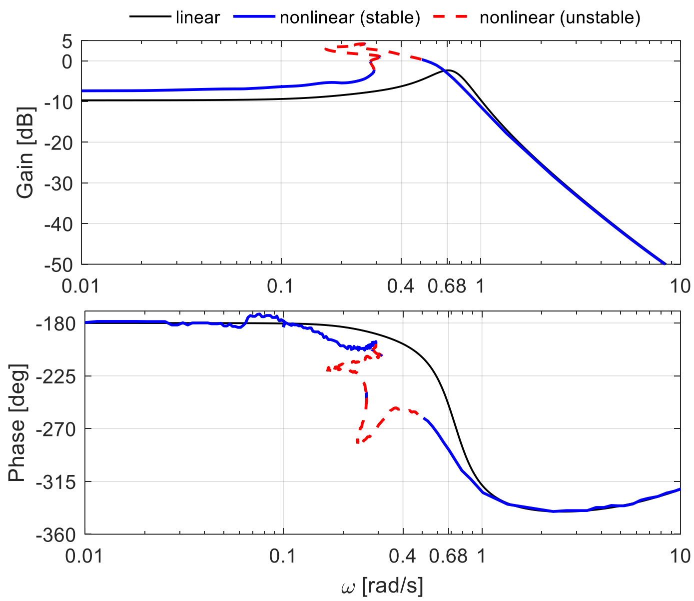

Fig. 5 GTT linear vs nonlinear α-to-δ_e frequency responses – A = 20º

To verify the effectiveness of the escape manoeuvre and highlight the need for our proposed nonlinear frequency method, we compare the time simulation of the forced nonlinear aircraft model in Fig. 6 at two forcing frequencies of 0.68 rad/s and 0.40 rad/s. The former is the resonance frequency indicated by the linear frequency response, and the latter lies in the region where only unstable solutions exist according to the nonlinear Bode plot. It can be seen that the aircraft diverges when subjected to the 0.40 rad/s forcing, whereas if the higher frequency predicted by linear analysis is used, then the response is stable and has a smaller amplitude. This feature is correctly predicted by nonlinear frequency analysis. Linear analysis is therefore not suitable for determining the optimal forcing frequency for deep stall recovery. Furthermore, conventional bifurcation analysis like in Fig. 3 only shows steady-state behaviour, which is inadequate for revealing the stability characteristics of forced responses.

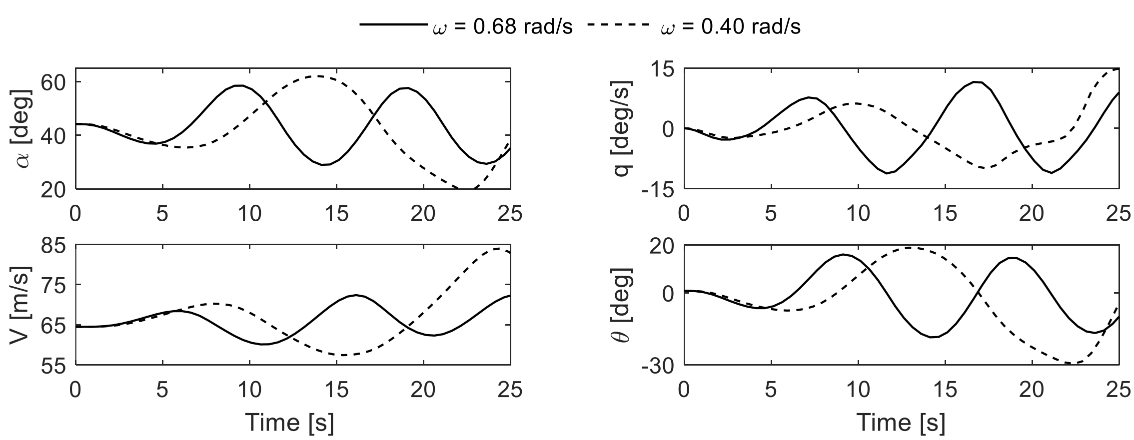

Fig. 6 Forced responses. $\delta_e = 20\ sin\ \omega t$ (deg).

The rigid-body dynamics of an open-loop aircraft are usually separated into the short-period (fast) mode and the phugoid (slow) mode, which should be distinctly visible in the Bode plot and separated by an order of magnitude in frequency. This is not the case as seen in Fig. 5 as well as Fig. 7, where only one peak is visible. At such a high angle-of-attack, the frequency separation between the two modes is greatly reduced, and the aircraft response no longer resembles the conventional short-period and phugoid dynamics seen at lower angles-of attack. Comparing the step further highlights this feature. Fig. 8a is an example of a typical step response in normal flight, where the fast and slow dynamics are clearly visible. At an angle-of-attack in the deep stall region like in Fig. 8b, the dynamics is remarkably different with only one apparent mode.

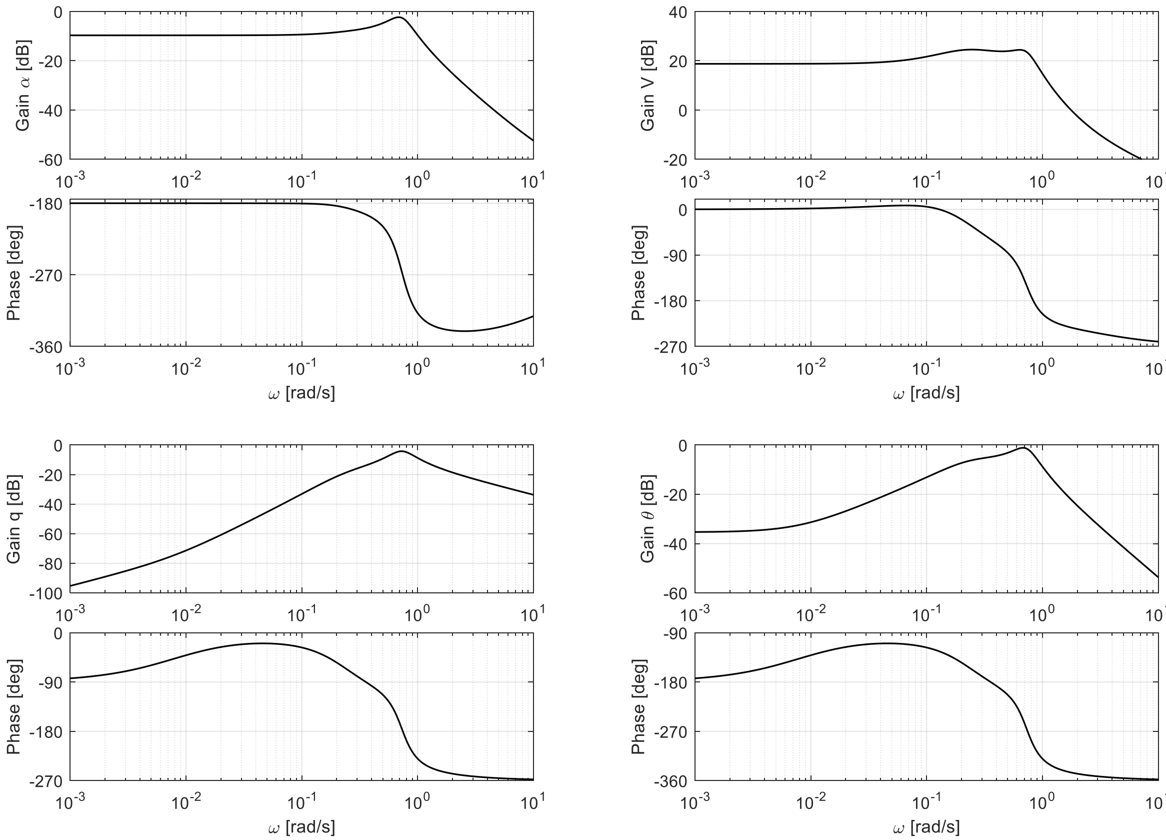

Fig. 7 Linear frequency responses at deep stall (δ_e = 0º). Natural frequencies: 0.23 and 0.73 rad/s.

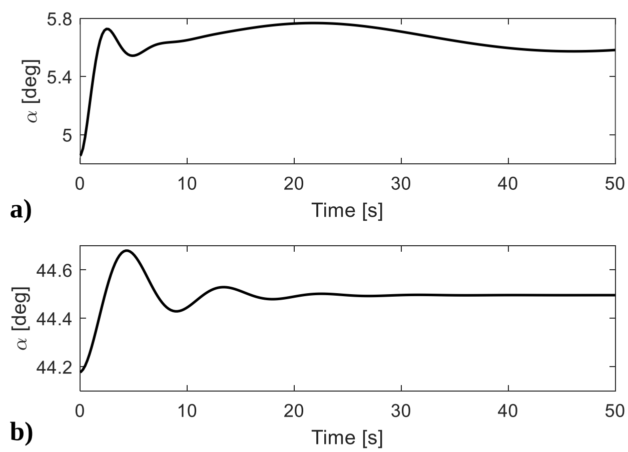

Fig. 8 Elevator step responses: 17º to 16º (a) and 0º to –1º (b).

Finally, the movement of the linear poles from low to high angles-of-attack is examined in Fig. 9. This verifies that as the angle-of-attack increases, both the short-period and phugoid roots move toward each other, leading to the reduced frequency separation observed in the Bode plots and the time simulation. The corresponding linear transfer functions state-space matrices are provided in the appendix. Since the reduced frequency separation is significant, it can be said that past studies that only examined the short period dynamics on 2nd-order longitudinal models [6-8] may give inaccurate results. Furthermore, any controller designed for normal flight will also be expected to have significantly reduced performance in this deep stall region due to the unconventional open-loop dynamics.

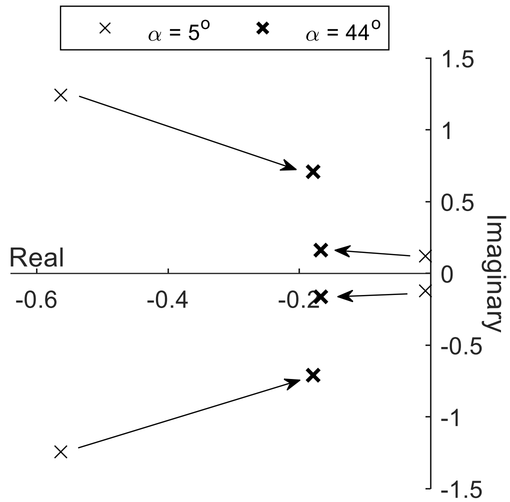

Fig. 9 Pole positions: normal flight vs deep stall.

Scope of the final paper: the paper in its current form can be considered final. However, we are also exploring the use of eigenstructure analysis to gain a better understanding of how the conventional fast and slow modes transform into the single peak observed in the frequency response at deep stall. The insight gained from this methodology can improve our understanding of the flight dynamics at high angles-of-attack and potentially be used to aid controller design. Reference [26] provides the first application of eigenstructure analysis in a flight dynamics context, although the study in reference [26] included lateral-directional coupling, which made the stall and post-stall upset behaviours more difficult to interpret. These results will be included in the final paper if they are found to be a valuable addition to the discussion.

V. Conclusion

Previous research into deep stall recovery has encountered numerous difficulties due to the nonlinear nature of flight dynamics at high angle-of-attack. Many promising procedures also require a dynamic (nonstationary) approach, which further stretches the limits of existing analysis techniques and highlights the need for a more nonlinear-based method. In this note, we have shown that bifurcation methods implemented in the form of nonlinear frequency analysis can facilitate a systematic study to identify possible recovery manoeuvres. Despite very limited pitch control authority at high angles-of-attack, it is still possible to initiate recovery by forcing the pitch control device at one of the nonlinear resonant frequencies. This manoeuvre can induce a large-amplitude oscillation that eventually rocks the aircraft out of the previously unrecoverable deep stall. These large-amplitude resonances are reflected as asymptotically unstable solutions, and their frequencies can be identified using the proposed method. On the other hand, the resonance frequency predicted by linear analysis is incorrect, and relying on linear-based result may lead to unsuccessful recovery due to being insufficiently close to the true resonance peak. It was also found that at high angles-of-attack, the frequency separation between the conventional short-period and phugoid modes is significantly reduced, leading to non-conventional dynamics that resemble only one single mode.

Acknowledgements

The first author is partially supported by the University of Bristol's Alumni Grant. We would like to thank NASA Langley Research Center for providing data of the GTT model.

References

1. Trubshaw, E. B. "Low Speed Handling with Special Reference to the Super Stall", *Journal of the Royal Aeronautical Society*, Vol. 70, No. 667, 1966, pp. 695-704.
doi: 10.1017/S0001924000057110

2. Iloputaife, O. I. "Design of Deep Stall Protection for the C-17A", *Journal of Guidance, Control, and Dynamics*, Vol. 20, No. 4, 1997, pp. 760-767.
doi: 10.2514/2.4109

3. Nguyen, L. T., Ogburn, M. E., Gilbert, W. P., Kibler, K. S., Brown, P. W., and Deal, P. L. "Simulator Study of Stall/Post-Stall Characteristics of a Fighter Airplane with Relaxed Longitudinal Static Stability," *NASA Technical Paper 1538*. NASA, Langley Research Center, Hampton, Virginia, 1979.

4. Avanzini, G., and Matteis, G. d. "Bifurcation Analysis of a Highly Augmented Aircraft Model", *Journal of Guidance, Control, and Dynamics,* Vol. 20, No. 4, 1997, pp. 754-759.
doi: 10.2514/2.4108

5. Gousman, K., Loschke, R., Rooney, R., and Juang, J. "Aircraft deep stall analysis and recovery", *18th Atmospheric Flight Mechanics Conference*, AIAA Paper AIAA-91-2888-CP, 1991.
doi: 10.2514/6.1991-2888

6. Montgomery, R. C., and Moul, M. T. "Analysis of deep-stall characteristics of T-tailed aircraft configurations and some recovery procedures", *Journal of Aircraft,* Vol. 3, No. 6, 1966, pp. 562-566.
doi: 10.2514/3.43777

7. Kolb, S., Hétru, L., Faure, T. M., and Montagnier, O. "Nonlinear analysis and control of an aircraft in the neighbourhood of deep stall", *ICNPAA 2016 World Congress*, ICNPAA, Vol. 1798, No. 1, pp. 020080, 2016.
doi: 10.1063/1.4972672

8. Wu, D., Chen, M., and Ye, H. "Analysis and Recovery of Aircraft Deep-Stall Phenomena Using Bifurcation Analysis", *IEEE Access*, Vol. 8, 2020, pp. 29319-29333.
doi: 10.1109/ACCESS.2020.2972570

9. Evangelou, L. D., Self, A. W., Allen, J. E., and Lo, S. "Trimmed deep stall on the F-16 Fighting Falcon", *The Aeronautical Journal,* Vol. 105, No. 1054, 2001, pp. 679-683.
doi: 10.1017/S0001924000012720

10. Thomas, P. R., Bullock, S., Bhandari, U., and Richardson, T. S. "Fixed-wing approach techniques for complex environments", *The Aeronautical Journal,* Vol. 119, No. 1218, 2015, pp. 999-1016.
doi: 10.1017/S0001924000004292

11. Cunis, T., Condomines, J.-P., and Burlion, L. "Sum-of-Squares Flight Control Synthesis for Deep-Stall Recovery", *Journal of Guidance, Control, and Dynamics,* Vol. 43, No. 8, 2020, pp. 1498-1511.
doi: 10.2514/1.G004753

12. Cunis, T., Condomines, J.-P., Burlion, L., and Cour-Harbo, A. l. "Dynamic Stability Analysis of Aircraft Flight in Deep Stall", *Journal of Aircraft,* Vol. 57, No. 1, 2020, pp. 143-155.
doi: 10.2514/1.C035455

13. Cunningham, K., Shah, G. H., Frink, N. T., McMillin, S. N., Murphy, P. C., Brown, F. R., Hayes, P. J., Shweyk, K. M., and Nayani, S. N. "Preliminary Test Results for Stability and Control Characteristics of a Generic T-tail Transport Airplane at High Angle of Attack", *2018 AIAA Atmospheric Flight Mechanics Conference*, AIAA Paper AIAA-2018-0529, 2018.
doi: 10.2514/6.2018-0529

14. Cunningham, K., Shah, G. H., Hill, M. A., Pickering, B. P., Litt, J. S., and Norin, S. "A Generic T-tail Transport Airplane Simulation for High-Angle-of-Attack Dynamics Modeling Investigations", *2018 AIAA Modeling and Simulation Technologies Conference*, AIAA Paper AIAA-2018-1168, 2018.
doi: 10.2514/6.2018-1168

15. Cunningham, K., Shah, G. H., Murphy, P. C., Hill, M. A., and Pickering, B. "Pilot Sensitivity to Simulator Flight Dynamics Model Formulation for Stall Training", *AIAA Scitech 2019 Forum*, AIAA Paper AIAA-2019-0717, 2019.
doi: 10.2514/6.2019-0717

16. Advani, S., and Field, J. "Upset Prevention and Recovery Training in Flight Simulators", *AIAA Modeling and Simulation Technologies Conference*, AIAA Paper AIAA-2011-6698, 2011.
doi: 10.2514/6.2011-6698

17. Fucke, L., Biryukov, V., Grigorev, M., Rogozin, V., Groen, E., Wentink, M., Field, J., Soemarwoto, B., Abramov, N., Goman, M., and Khrabrov, A. "Developing Scenarios for Research into Upset Recovery Simulation", *AIAA Modeling and Simulation Technologies Conference*, AIAA Paper AIAA-2010-7794, 2010.
doi: 10.2514/6.2010-7794

18. Carroll, J. V., and Mehra, R. K. "Bifurcation Analysis of Nonlinear Aircraft Dynamics", *Journal of Guidance, Control, and Dynamics,* Vol. 5, No. 5, 1982, pp. 529-536.
doi: 10.2514/3.56198

19. Goman, M. G., Zagainov, G. I., and Khramtsovsky, A. V. "Application of Bifurcation Methods to Nonlinear Flight Dynamics Problems", *Progress in Aerospace Sciences,* Vol. 33, No. 9-10, 1997, pp. 539-586.
doi: 10.1016/S0376-0421(97)00001-8

20. Richardson, T., Lowenberg, M., Di Bernardo, M., and Charles, G. "Design of a Gain-Scheduled Flight Control System Using Bifurcation Analysis", *Journal of Guidance, Control, and Dynamics,* Vol. 29, No. 2, 2006, pp. 444-453.
doi: 10.2514/1.13902

21. Gill, S. J., Lowenberg, M. H., Neild, S. A., Crespo, L. G., and Krauskopf, B. "Impact of Controller Delays on the Nonlinear Dynamics of Remotely Piloted Aircraft", *Journal of Guidance, Control, and Dynamics,* Vol. 39, No. 2, 2016, pp. 292-300.
doi: 10.2514/1.G001222

22. Nguyen, D. H., Lowenberg, M. H., and Neild, S. A. "Frequency-Domain Bifurcation Analysis of a Nonlinear Flight Dynamics Model", *Journal of Guidance, Control, and Dynamics,* Vol. 44, No. 1, 2021, pp. 138-150.
doi: 10.2514/1.G005197

23. Nguyen, D. H., Lowenberg, M. H., and Neild, S. A. "Effect of Actuator Saturation on Pilot-Induced Oscillation: a Nonlinear Bifurcation Analysis", *Journal of Guidance, Control, and Dynamics,* Vol. 44, No. 5, 2021, pp. 1018-1026.
doi: 10.2514/1.G005840

24. Coetzee, E., Krauskopf, B., and Lowenberg, M. H. "The Dynamical Systems Toolbox: Integrating AUTO into Matlab", *16th US National Congress of Theoretical and Applied Mechanics*, USNCTAM Paper USNCTAM2010-827, 2010.

25. Doedel, E. J. "*AUTO-07P, Continuation and Bifurcation Software for Ordinary Differential Equations, Ver. 07P*", http://www.macs.hw.ac.uk/~gabriel/auto07/auto.html [retrieved 8 April 2021].

26. Perez, M. M., and Lowenberg, M. H. "Eigenvector similarity metrics for the identification and quantitative study of aircraft dynamic modes", *AIAA Scitech 2021 Forum*, AIAA Paper AIAA-2021-1724, 2021. doi: 10.2514/6.2021-1724

Appendix. Linear approximation at deep stall

The following state-space model was obtained from the trimmed aircraft in deep stall at full nose-down stabilator (-10^o), δ_e = 0º, T = 0 N, cg = 40% MAC, α = 44.2 deg, V = 64.5 m/s, q = 0 deg/s, and θ = 0.87 deg. Note that α, q, and θ have units rad/s or rad in the state-space matrices.

$$\boldsymbol{x} = [\alpha, V, q, \theta]^T \qquad \boldsymbol{u} = \delta_e$$

$$\boldsymbol{A} = \begin{bmatrix} -0.13858 & -0.00343 & 0.92943 & 0.10426 \\ -7.14144 & -0.20869 & -4.27044 & -7.13799 \\ -0.62887 & 2.74314e-06 & -0.34515 & -6.30705 \\ 0 & 0 & 1 & 0 \end{bmatrix}$$

$$\boldsymbol{B} = \begin{bmatrix} -0.00024411 \\ -0.011471 \\ -0.0035998 \\ 0 \end{bmatrix}$$

$$\boldsymbol{C} = \begin{bmatrix} 1 & 0 & 0 & 0 \\ 0 & 1 & 0 & 0 \\ 0 & 0 & 1 & 0 \\ 0 & 0 & 0 & 1 \end{bmatrix}$$

$$\boldsymbol{D} = \begin{bmatrix} 0 \\ 0 \\ 0 \\ 0 \end{bmatrix}$$

Linear transfer functions:

$$\frac{\alpha(s)}{\delta_e(s)} = \frac{-0.013986\,(s+13.77)\,(s^2+0.3328s+0.04953)}{(s^2+0.3345s+0.05439)\,(s^2+0.3579s+0.5347)} \quad \left(\frac{deg}{deg}\right)$$

$$\frac{V(s)}{\delta_e(s)} = \frac{-0.011471\,(s-2.572)\,(s+1.461)\,(s+0.1019)}{(s^2+0.3345s+0.05439)\,(s^2+0.3579s+0.5347)} \quad \left(\frac{m/s}{deg}\right)$$

$$\frac{q(s)}{\delta_e(s)} = \frac{-0.20625s\,(s+0.2965)\,(s+0.008109)}{(s^2+0.3345s+0.05439)\,(s^2+0.3579s+0.5347)} \quad \left(\frac{deg/s}{deg}\right)$$

$$\frac{\theta(s)}{\delta_e(s)} = \frac{-0.20625s\,(s+0.2965)\,(s+0.008109)}{(s^2+0.3345s+0.05439)\,(s^2+0.3579s+0.5347)} \quad \left(\frac{deg}{deg}\right)$$